

# A Neuromorphic VLSI Model of Grid Cells in the Echolocating Bat

Timothy K. Horiuchi

Electrical and Computer Engineering Department  
Institute for Systems Research  
University of Maryland  
College Park, MD, 20742, USA  
timmer@umd.edu

Tarek M. Massoud

Electrical and Computer Engineering Department  
University of Maryland  
College Park, MD 20742, USA  
tmassoud@umd.edu

**Abstract**— Neurophysiological experiments in the hippocampal formation of echolocating bats have found grid cells (thought to be used for odometry) as in other mammals, but without continuous theta frequency oscillations (~8 Hz) prominent in other mammals. We describe a ‘theta-free’ model of grid cell property creation for echolocating bats that is amenable to VLSI implementation of hippocampal models of spatial navigation. We demonstrate a hybrid implementation of a 2-D model (microcontroller and neuromorphic VLSI) using recorded input from a sonar system.

## I. INTRODUCTION

Since the discovery of ‘place’ cells in the rat [1], the spatial odometry system in mammals (especially in rats) has been heavily studied, resulting in additional discoveries of cells that code for head-direction in world coordinates [2] and ‘grid’ cells that fire at the vertices of a triangular grid pattern overlaid on the environment [3]. A prominent feature of both grid and place cells in the rat is the local field potential oscillations in the theta frequency band (6-10 Hz) and that the spiking activity of these cells are also modulated at these frequencies.

Many different models for the creation of grid cell properties have been proposed, with most falling into one of two major categories: oscillatory-interference models that use the relative phase of multiple theta frequency oscillators (e.g., [4]) and 2D attractor networks that create a triangular grid pattern of activity on a neural sheet using local synaptic projection fields (e.g., [5]). In these attractor models, theta oscillation is not used to create the fields, however, theta modulation of firing can be injected into the activity and still explain much of the experimental data. Although these two classes of models are dramatically different and naturally explain different aspects of the biological data, neurophysiological evidence has yet to rule out either class (for review, see [6]).

In the oscillatory-interference models, translational motions of the animal result in persistent phase changes of oscillators (i.e., memory of position), resulting in position-dependent phase-synchronization at downstream grid cells. Notably, with this model, it is possible to build a single isolated grid cell at a given frequency using minimal synaptic connectivity. A requirement for good performance, however, is that the oscillators have very good phase stability.

In the attractor network models, translational motions of the animal result in an asymmetrical pattern of recurrent activity, resulting in a global shift in the phase of the grid activity pattern on the sheet (i.e., memory of position). In this model, it is not possible to create a single grid cell at a given frequency because the grid pattern emerges from the network. Due to the high neuron count, extensive synaptic interconnectivity, and complex pattern-movement wiring, this model is challenging for neuromorphic VLSI implementation unless some simplifications are made [7]. Fabrication mismatch readily creates drift and trapping in local minima.

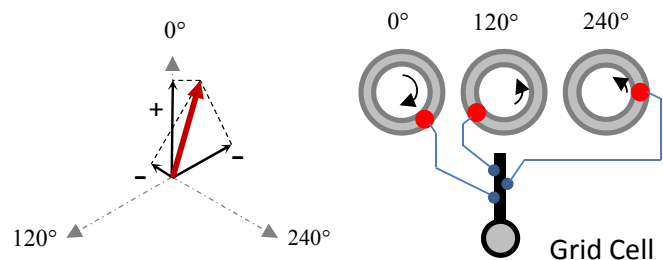


Fig. 1. Left: A two-dimensional movement vector (thick red arrow) is projected onto each of the three ring integrator orientations. The resulting vectors are then translated into a ring activity-bump rotational phase rate. Projection vectors with ‘+’ signs produce positive phase rotations and vectors with ‘-’ signs produce negative phase rotations. Note that these vectors are defined in the world frame of reference (allocentric). While not simulated here, this could be accomplished using a speed-modulated, head-direction (HD) cell [2] that has trigonometrically-appropriate, synaptic projection strengths onto cells that control each ring-integrator’s rotation rate. Right: Neurons from each integrator representing a particular phase, project activity to a single grid cell configured to detect a three-way coincidence using saturating synapses.

Recent neurophysiological experiments have discovered place cells in the big brown bat [8] and both place cells and grid cells in the Egyptian fruit bat [9]. While these place and grid fields are similar to those in the rat, continuous theta oscillations are not present, suggesting that theta oscillations are not fundamental to the creation of grid cell or place cell formation in bats. In contrast, transient theta oscillations occur in 1-2 sec bouts mostly during short periods during active echolocation behavior [8].

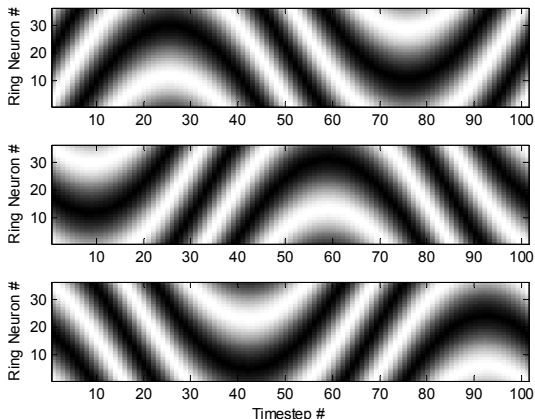


Fig. 2. Evolution of three ring integrator networks (tuned to 0, 120, and 240 degrees from top to bottom) as a simulated bat travels in a complete circle. The scaling parameter from translational speed to rotation rate are those used for generating Fig. 2 (left). White denotes the strongest activity and black denotes no activity.

Our model for the bat grid cells is based on a model proposed by [10] where non-oscillatory ‘stripe cells’ replace paired, interfering oscillators. In our model, the stripe cells are implemented as a ring-integrator network that moves a self-sustaining “bump” of neural activity cyclically in response to *translational* movements of the animal. This proposed ring-integrator is identical to network models of the head-direction cell system except that it is driven by translational movement inputs scaled by the animal’s speed *and* heading (i.e., speed-modulated head-direction cells).

Travel in two-dimensions is represented by three ring-integrator networks that represent the projection of the animal’s allocentric (i.e., world referenced) velocity vector onto reference vectors pointing in the 0, 120, and 240 degree orientations (Fig. 1, left). As the animal moves in different directions, the activity bumps on the three rings rotate at different speeds and in different directions.

A grid cell receives its inputs from one location (i.e., phase) on each ring (Fig 1, right), creating a maximum at spatial locations that occur on a triangular grid. To create grid cells of different spatial frequencies, we create new triplets of ring-integrators that have a different scaling between animal speed and bump rotation rate.

This model network has a number of desirable properties in the context of the current scientific literature and from a neuromorphic VLSI perspective. First, the model does not use theta oscillations to create the grid pattern, consistent with the bat hippocampal data. Second, unlike the 2D attractor network models for grid cells, a large, specifically-wired 2D network to

create and move the triangular grid of activity is not needed. Third, the model uses the same ring-integrator network as is postulated for the head-direction cell system.

In the attractor-network model of grid cells, the memory of the animal’s position is stored in the combination of phases of the activity patterns found on the grid cells of different spatial frequencies. In our model, like the phase interference model, the memory of the animal’s position is stored in the combination of phases of the different ring O/I networks of different spatial frequencies (upstream of the grid cells), which likely represents a much smaller number of neurons than would be necessary for the attractor network model. Like the phase interference model, the grid cells only need to be driven by the inputs of the ring-integrator networks, allowing the properties of a given grid cell to be independent of neighboring grid cells. This arrangement avoids boundary condition effects that arise in the attractor networks.

## II. SOFTWARE MODELING

### A. Ring Integrators

The ring-integrator networks were simulated in MATLAB® to be 36 non-spiking neurons per ring with analog activation values. The activity bump was Gaussian with a sigma of 1.9 radians. A specific movement neural network was not implemented; the phase (i.e., position of the Gaussian) was simply advanced with time according to the direction and speed of travel. Using a simulated bat following a specified trajectory, the velocity vector was projected onto each of the three ring-integrator orientation vectors (see Fig 1.) and the magnitude of the projections were scaled into the rotation rate for each ring-integrator network. An example of the evolution of ring activity is shown in Fig. 2 where a simulated bat flies in a circle. Note that the starting and ending phase for all three integrators is the same. Changing the scaling factor produces different spatial frequency grid fields.

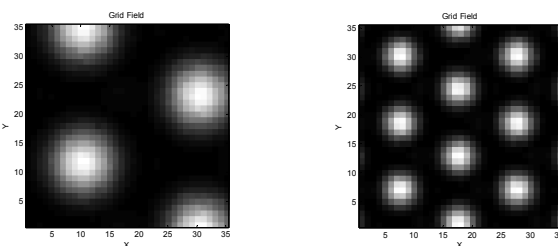


Fig. 3. Two examples of spatial grid fields produced by a single grid cell of a simulated bat moved across the environment. Different spatial scales are produced by scaling the translation from movement speed to ring integrator phase rate.

### B. Simulated Grid Cells

Although earlier models from Burgess and colleagues used a summation of the three orientation inputs to drive the grid cell, *multiplication* of the three inputs that target different dendritic branches [4] appears to fit the data better [11]. In fact, logarithmic compression (i.e., saturation of the dendritic contributions) of the individual inputs prior to summation at the soma can produce this multiplicative effect and is very

close to a logical AND of the inputs. Fig. 3 shows two examples of spatial grid patterns resulting from two ring integrator speed scaling factors.

### III. A NEUROMORPHIC VLSI GRID CELL

#### A. A Hybrid Implementation Using VLSI Hardware

In the previous section, the model was simulated in MATLAB® to provide the cleanest definition of the model. In this section, we demonstrate the implementation of the grid cell calculation on a neuromorphic VLSI circuit using saturating *synapses* in a single compartment neuron model to mimic the multiplicative model (using the concept of *dendritic branch saturation*). The ring integrator portion of the model was implemented on an 18F series PIC® microcontroller with motion signals coming from a

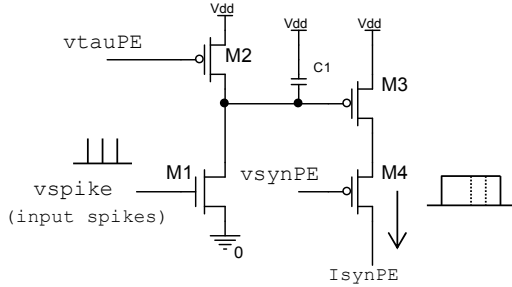


Fig. 4. A simple digital pulse-extension synapse that produces a long duration current pulse of “constant” current. The output current level ( $I_{synPE}$ ) is controlled by  $v_{synPE}$  and the duration is controlled by  $v_{tauPE}$ . Input spikes that arrive before the end of the previous current pulse “reset” the pulse timing to extend the duration of the pulse. This saturating behavior enables the logical AND function desired in the grid cell computation. The transistor sizes were identical and were fabricated at  $2.5\mu\text{m}/2.5\mu\text{m}$ .

computer. The microcontroller provided neuron outputs for the three ring-integrator networks (corresponding to one spatial frequency) as spike trains that were transmitted to a neuromorphic VLSI neuron chip. The neuromorphic VLSI chip was fabricated in a commercially-available  $0.5\mu\text{m}$  CMOS process for general purpose neuromorphic education and research.

As the simulated bat moves around in the environment, a triple coincidence between the three ring phases occurs periodically in space. To detect the coincidence, we used a “pulse-extension” synapse circuit [12] (Fig. 4.) that extends the short duration spike ( $\sim 1$  microsecond) used in our inter-chip communication system into a longer, square-wave current pulse. This current is translated into a conductance at the neuron circuit. Additional spikes arriving before the end of the pulse will reset the timing of the pulse and extend the duration without increasing the current level. The currents from the three synapse circuits are summed, resulting in a combined conductance that simulates parallel conductances.

#### B. Neuron Circuit

The neuron circuit (Fig. 5) is a subthreshold-regime, current-mode, conductance-based neuron design (similar to [12]). In this design, the membrane potential is represented

as a current ( $I_{mem\_ss}$ , drain current of M10) with a current threshold for firing a spike (drain current of M11). The excitatory input current acts as a conductance, pulling the membrane “potential” up above the threshold level. The

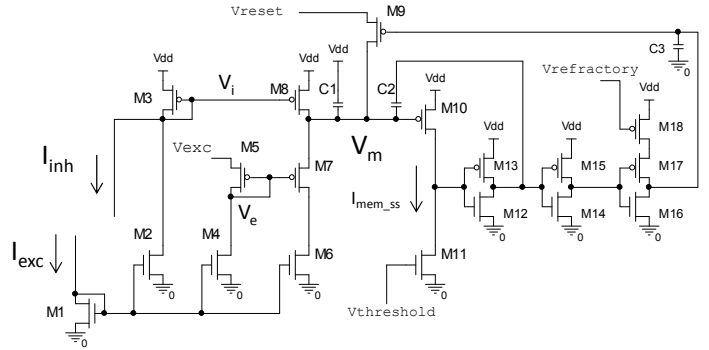


Fig. 5. The neuron circuit used to convert excitatory and inhibitory input currents into conductance. Transistor sizes were all  $2.5\mu\text{m}/2.5\mu\text{m}$  except for M6 which was  $3.2\mu\text{m}/2.0\mu\text{m}$ .  $C1=500\text{fF}$ .  $C2$  and  $C3=30\text{fF}$ .  $I_{inh}$  raises  $V_m$  and  $I_{exc}$  lowers  $V_m$ .  $V_{exc}$  controls the excitatory reversal potential and  $V_{reset}$  controls the post-firing reset level.

inhibitory current also acts as a conductance, pulling the membrane below the firing potential. This competition determines the steady-state value of the membrane “potential” and thus determines if the neuron will fire a spike or not. The current representing the membrane “potential” reaches a steady-state value given by:

$$I_{mem\_ss} = I_o \cdot e^{\frac{\kappa(V_{dd}-v_{exc})}{V_T}} \left( \frac{I_{exc}}{I_{exc} + I_{inh}} \right) \quad (1)$$

Where  $I_o$  represents the subthreshold scaling current and  $\kappa$  represents the gate capacitive coupling factor. Because the

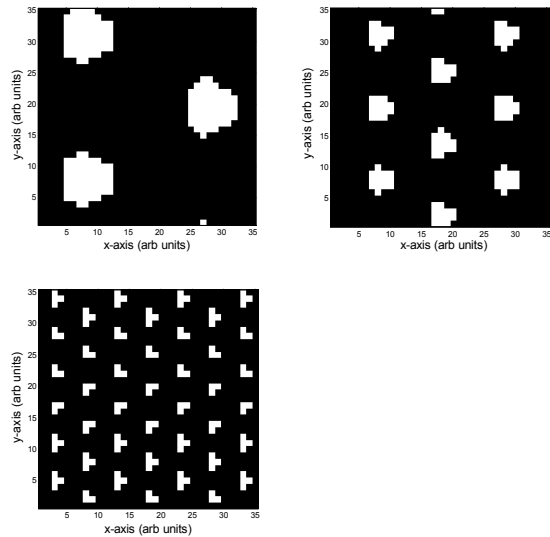


Fig. 6. Spatial grid patterns generated by a neuromorphic VLSI neuron driven by three saturating synapses (VLSI) to detect a three-way coincidence of particular phases from three ring-integrator networks (microcontroller). Three spatial frequencies are demonstrated by changing the scaling factor between movement speed (e.g., m/sec) and the phase rate (e.g., rad/sec)

three synapses saturate, we can select a threshold current

(controlled by  $V_{threshold}$ ) and inhibitory current to only produce a spike if all three inputs are active. In this circuit, the capacitor C1 only acts as a lowpass filter.

### C. Grid Cells

In our implementation of the model, using a single compartment VLSI neuron, saturating synapses are used to mimic the effect of separate dendritic compartments. The result is close to a logical AND (to approximate the multiplicative solution). To demonstrate the use of this neuromorphic VLSI implementation and to visualize the firing field of the grid cell, we moved the position of simulated bat to all locations in a square grid to produce the grid field pattern seen in rat experiments (Fig. 6).

### D. Sonar-Driven Grid Cells

To demonstrate the system with a natural spatial movement signal closer to our intended application, we used a single sonar transducer observing a moving pole to simulate an aerial vehicle (e.g., a robot bat) using a *fixed* pole as a position reference. The sonar samples were at 10 Hz and the range rate was fed into the ring integrator network assuming a fixed angle (zero radians).

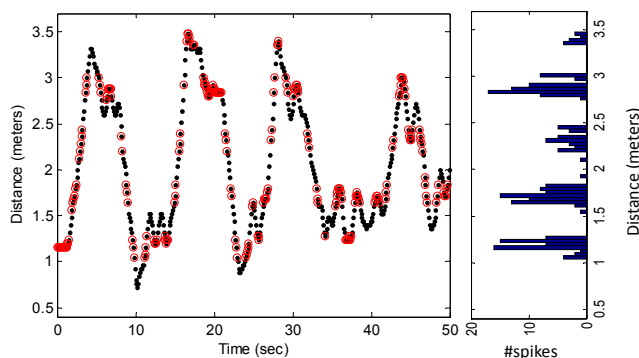


Fig. 7. Sonar-driven grid cell activity. Left: A sonar transducer measures the distance to a moving pole (black dots). The range rate drives the ring O/I simulation that drives the VLSI grid cell. Red circles indicate where the grid cell fired. As the simulated hovering bat moves back and forth, it crosses five different vertices of its grid field. Right: Histogram of grid cell responses shows the periodic structure of the grid field.

The initial integrator phases were selected such that the line of travel aligned with the nodes of the grid field.

## IV. DISCUSSION

The use of the ring-integrator networks to replace pairs of interfering theta oscillators provides a much simpler model for the bat grid cell system, retaining many of the desirable properties of the original phase-interference model, without resorting to a full 2-D attractor circuit as in [7]. Two-dimensional movements of the animal are implemented as one-dimensional movements on multiple rings, arguably simplifying the required network. While this paper only explored the grid cell portion of the model in silicon, implementing a spiking neuron-based ring-integrator network

with good rotational control has already been demonstrated for a neuromorphic VSI head-direction cell system [14].

Recent work [15] has shown that large numbers of grid cells at each frequency are not necessary to generate compact place fields. This model allows for targeted construction of grid field properties for efficient neuromorphic VLSI-based implementations of place cells in the hippocampus that may require a diversity of grid cell inputs. Perhaps most interesting for both VLSI and biological implementation, expansion of the model to 3-D only requires one additional ring-integrator.

### ACKNOWLEDGMENT

We thank Ralph Etienne-Cummings and Jon Tapson for inspiration during the 2012 Telluride Neuromorphic Cognition Engineering Workshop and Cynthia Moss for discussions of the big brown bat experiments. We also thank MOSIS for their support of silicon fabrication for educational purposes.

### REFERENCES

- [1] J. O'Keefe and J. Dostrovsky, "The hippocampus as a spatial map: preliminary evidence from unit activity in the freely moving rat", *Brain Res.* vol. 34, pp. 171-175, 1971.
- [2] J. B. Ranck Jr., "Head direction cells in the deep cell layers of dorsal presubiculum in freely moving rats", *Soc. Neurosci. Abstr.* 10: p. 599, 1984.
- [3] T. Hafting, M. Fyhn, S. Molden, M. B. Moser, and E. I. Moser, "Microstructure Of A Spatial Map In The Entorhinal Cortex," *Nature*, vol. 436, pp. 801-806, 2005.
- [4] N. Burgess, Barry, J. O'Keefe, "An oscillatory interference model of grid cell firing", *Hippocampus*, 17(9), pp. 801-812, 2007
- [5] M. C. Fuhs and D. S. Touretzky, "A spin glass model of path integration in rat medial entorhinal cortex", *J Neurosci* vol. 26, pp. 4266-4276, 2006.
- [6] J. Knierim and K. Zhang, "Attractor Dynamics of Spatially Correlated Neural Activity in the Limbic System", *Annu. Rev. Neurosci.* Vol. 35, pp. 267-86, 2012.
- [7] T. M. Massoud and T. K. Horiuchi, "A Neuromorphic VLSI Grid Cell System". *IEEE Intl Symposium on Circuits and Systems (Systems (ISCAS 2012)*, May 2012, Seoul, Korea. pp. 2421-2424. 2012.
- [8] N. Ulanovsky and C. F. Moss, "Hippocampal cellular and network activity in freely moving echolocating bats", *Nature Neuroscience* vol. 10, pp. 224-233, 2007.
- [9] M. M. Yartsev, M. P. Witter, and N. Ulanovsky, "Grid cells without theta oscillations in the entorhinal cortex of bats", *Nature* vol. 479, pp. 103-107, 2011.
- [10] H. Mhatre, A. Gorchetchnikov, and S. Grossberg, "Grid cell hexagonal patterns formed by fast self-organized learning within entorhinal cortex", *Hippocampus*, 22(2), pp. 320-334, 2012.
- [11] M. Hasselmo, L. Giocomo, E. Zilli, "Grid cell firing may arise from interference of theta frequency membrane potential oscillations in single neurons", *Hippocampus*, 17(12), pp. 1252-1271, 2007.
- [12] J. V. Arthur and K. Boahen, "Silicon Neurons That Inhibit To Synchronize," in *Proc. International Symposium on Circuits and Systems (ISCAS 2006)*, Island of Kos, Greece, 2006.
- [13] T. K. Horiuchi, C. Bansal, and T. M. Massoud, "Binaural intensity comparison in the echolocating bat using synaptic conductance", *Proc. Intl Symp Circ Sys (ISCAS 2009)* pp. 2153-2156, 2009.
- [14] T. M. Massoud and T. K. Horiuchi, "A Neuromorphic VLSI Head Direction Cell System," *Circuits and Systems I: Regular Papers, IEEE Transactions on*, vol. 99, 2010.
- [15] A. Mathis, A. V. Herz, and M. Stemmler, "Optimal population codes for space: grid cells outperform place cells", *Neural Computation*, 24(9), pp. 2280-2317, 2012.